Common variants in 22 loci are associated with QRS duration and cardiac ventricular conduction

Nona Sotoodehnia[1,2,78]*, Aaron Isaacs[3,4,78], Paul I W de Bakker[5–8,78], Marcus Dörr[9,78], Christopher Newton-Cheh[10–12,78], Ilja M Nolte[13,78], Pim van der Harst[14,78], Martina Müller[15–17,78], Mark Eijgelsheim[18,78], Alvaro Alonso[19,78], Andrew A Hicks[20,78], Sandosh Padmanabhan[21,78], Caroline Hayward[22,78], Albert Vernon Smith[23,24,78], Ozren Polasek[25,78], Steven Giovannone[26,78], Jingyuan Fu[13,27,78], Jared W Magnani[12,28], Kristin D Marciante[2], Arne Pfeufer[20,29,30], Sina A Gharib[31], Alexander Teumer[32], Man Li[33], Joshua C Bis[2], Fernando Rivadeneira[18,34], Thor Aspelund[23,24], Anna Köttgen[35], Toby Johnson[36,37], Kenneth Rice[38], Mark P S Sie[3], Ying A Wang[12,39], Norman Klopp[17], Christian Fuchsberger[20], Sarah H Wild[40], Irene Mateo Leach[14], Karol Estrada[34], Uwe Völker[32], Alan F Wright[22], Folkert W Asselbergs[13,14,41], Jiaxiang Qu[26], Aravinda Chakravarti[42], Moritz F Sinner[16], Jan A Kors[43], Astrid Petersmann[44], Tamara B Harris[45], Elsayed Z Soliman[46], Patricia B Munroe[36,37], Bruce M Psaty[2,47–49], Ben A Oostra[4,50], L Adrienne Cupples[12,39], Siegfried Perz[51], Rudolf A de Boer[14], André G Uitterlinden[18,34,52], Henry Völzke[53], Timothy D Spector[54], Fang-Yu Liu[26], Eric Boerwinkle[55,56], Anna F Dominiczak[21], Jerome I Rotter[57], Gé van Herpen[43], Daniel Levy[12,58], H-Erich Wichmann[15,17,59], Wiek H van Gilst[14], Jacqueline C M Witteman[18,52], Heyo K Kroemer[60], W H Linda Kao[33], Susan R Heckbert[2,47,49], Thomas Meitinger[29,30], Albert Hofman[18,52], Harry Campbell[40], Aaron R Folsom[19], Dirk J van Veldhuisen[14], Christine Schwienbacher[20,61], Christopher J O'Donnell[12,58], Claudia Beu Volpato[20], Mark J Caulfield[36,37], John M Connell[62], Lenore Launer[45], Xiaowen Lu[13], Lude Franke[27,63], Rudolf S N Fehrmann[27], Gerard te Meerman[27], Harry J M Groen[64], Rinse K Weersma[65], Leonard H van den Berg[66], Cisca Wijmenga[27], Roel A Ophoff[67,68], Gerjan Navis[69], Igor Rudan[40,70,71,78], Harold Snieder[13,54,78], James F Wilson[40,78], Peter P Pramstaller[20,72,73,78], David S Siscovick[2,47,78], Thomas J Wang[11,12,78], Vilmundur Gudnason[23,24,78], Cornelia M van Duijn[3,4,52,78], Stephan B Felix[9,78], Glenn I Fishman[26,78], Yalda Jamshidi[54,74,78], Bruno H Ch Stricker[18,34,43,52,75,78], Nilesh J Samani[76–78], Stefan Kääb[16,78] & Dan E Arking[42,78]

The QRS interval, from the beginning of the Q wave to the end of the S wave on an electrocardiogram, reflects ventricular depolarization and conduction time and is a risk factor for mortality, sudden death and heart failure. We performed a genome-wide association meta-analysis in 40,407 individuals of European descent from 14 studies, with further genotyping in 7,170 additional Europeans, and we identified 22 loci associated with QRS duration ($P < 5 \times 10^{-8}$). These loci map in or near genes in pathways with established roles in ventricular conduction such as sodium channels, transcription factors and calcium-handling proteins, but also point to previously unidentified biologic processes, such as kinase inhibitors and genes related to tumorigenesis. We demonstrate that *SCN10A*, a candidate gene at the most significantly associated locus in this study, is expressed in the mouse ventricular conduction system, and treatment with a selective *SCN10A* blocker prolongs QRS duration. These findings extend our current knowledge of ventricular depolarization and conduction.

The electrocardiographic QRS interval reflects ventricular depolarization, and its duration is a function of electrophysiological properties within the His-Purkinje system and the ventricular myocardium. A diseased ventricular conduction system can lead to life-threatening bradyarrhythmias, such as heart block, and tachyarrhythmias, such as ventricular fibrillation. Longer QRS duration is a predictor of mortality

and sudden death in the general population and in cohorts with hypertension and coronary artery disease[1–3]. In a population-based study, prolonged baseline QRS was associated with incident heart failure[4].

Twin and family studies suggest a genetic contribution to QRS duration, with heritability estimates of up to 40% (refs 5,6). Prior candidate gene and smaller genome-wide studies identified a limited

Figure 1 Manhattan plot. Manhattan plot showing the association of SNPs with QRS interval duration in a GWAS of 40,407 individuals. The dashed horizontal line marks the threshold for genome-wide significance ($P = 5 \times 10^{-8}$). Twenty loci (labeled) reached genome-wide significance. Two additional loci, *GOSR2* and *DKK1*, reached significance after genotyping of select SNPs in an additional sample of 7,170 individuals (see results section of the main text).
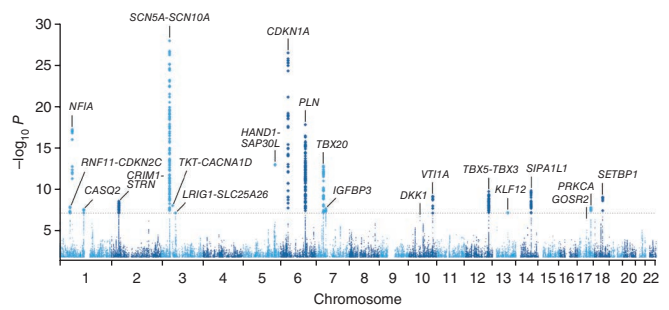
number of loci associated with QRS duration, supporting the hypothesis of the contribution of common genetic variation in QRS duration[7–9]. To identify additional loci and highlight physiologic processes associated with ventricular conduction, we performed a meta-analysis of 14 genome-wide association studies (GWAS) of QRS duration in a total of 40,407 individuals of European descent, where we adjusted the analyses for age, sex, height and body mass index (BMI) after appropriate sample exclusions (Online Methods). After an initial discovery phase, we further genotyped selected variants representing nine loci with P values ranging from $P = 1 \times 10^{-6}$ to $P = 5 \times 10^{-9}$ in an additional cohort of 7,170 European individuals.

RESULTS

Meta-analysis of genome-wide association results

We conducted meta-analyses for approximately 2.5 million SNPs in 40,407 individuals of European ancestry from 14 GWAS (**Supplementary Table 1a,b**). Overall, 612 variants in 20 loci exceeded our genome-wide significance P value threshold of $P = 5 \times 10^{-8}$ after adjusting for modest genomic inflation (genomic inflation factor (λ_{GC}) = 1.059) (**Fig. 1** and **Supplementary Fig. 1**). The loci associated with QRS interval duration are detailed in **Table 1** and **Supplementary Figure 2**, with the index SNP (representing the most significant association) labeled for each independent signal.

Across the genome, the most significant association for QRS interval duration (termed locus 1) was on chromosome 3p22 (**Fig. 2a**), where we identified six potentially independent association signals based on the linkage disequilibrium (LD) patterns in the HapMap European CEU population (pairwise r^2 among all index SNPs was <0.05). In conditional analyses where all six SNPs were included in the same regression model, there was compelling evidence that at least four SNPs from this region were independently associated with QRS duration (**Table 1**). Two of these associations were in or near *SCN10A*, which encodes a voltage-gated sodium channel. Variation at this locus was recently associated with QRS duration in two GWAS. The top SNP identified in those two studies, rs6795970, is in strong LD with our top signal, rs6801975 ($r^2 = 0.93$)[8,9]. Two additional signals were identified in *SCN5A*, a sodium channel gene adjacent to *SCN10A* (**Table 1**).

The second most significant locus (locus 2) was on chromosome 6p21 near *CDKN1A*, which encodes a cyclin-dependent kinase inhibitor. The *CDKN1A* locus was recently associated with QRS interval duration in an Icelandic population[9]. The index SNP in the prior report, rs1321311, is in strong LD with our top signal, rs9470361 ($r^2 = 0.88$). *CDKN2C*, which encodes another cyclin-dependent kinase inhibitor, is located in locus 15, which encompasses several other genes, including *C1orf185, RNF11* and *FAF1*.

Locus 3 on chromosome 6q22 contains the *PLN-SLC35F1-C6orf204-BRD7P3* cluster of genes. *PLN* encodes phospholamban, a key regulator of sarcoplasmic reticulum calcium reuptake. Significant associations were found in several other regions harboring calcium-handling genes, including locus 12 (*STRN-HEATR5B*), locus 16 (*PRKCA*) and locus 18 (*CASQ2*).

Locus 4 mapped to an intronic SNP in *NFIA*, which encodes a transcription factor. Several other significant loci also mapped in or near

genes encoding transcription factors, including locus 5 (*HAND1*), locus 6 (*TBX20*), locus 8 (*TBX5*), locus 9 (*TBX3*) and locus 19 (*KLF12*). Common variation in *TBX5* was recently associated with QRS duration[9]. The index signal in the prior report, rs3825214, was in moderate LD with our top signal, rs883079 ($r^2 = 0.67$).

Additional regions identified include locus 7 (*SIPA1L1*), locus 10 (*VTI1A*), locus 11 (*SETBP1*), locus 13 (*TKT-CACNA1D-PRKCD*), locus 14 (*CRIM1*), locus 17 (the nearest gene, *IGFBP3*, is 660 kb away) and locus 20 (*LRIG1*).

Collectively, the identified index SNPs across these 20 loci explained approximately 5.7% (± 2.3% (s.d.)) of the observed variance in QRS duration, consistent with a polygenic model in which each of the discovered variants exerts only a modest effect on QRS interval. None of these index SNPs showed a significant interaction with sex or age after Bonferroni correction (**Supplementary Table 2**). We observed moderate levels of heterogeneity of the effect ($25 < I^2 < 75$) for several index SNPs (**Table 1**). However, only *HAND1-SAP30L* showed significant evidence of heterogeneity using Cochran's Q test corrected for 23 independent genome-wide variants (Cochran's $P = 0.005$).

Extension of findings in an additional 7,170 individuals

Based on the discovery meta-analysis, we selected the index SNPs at four loci (loci 15, 17, 19 and 20) with P values ranging between $P = 5 \times 10^{-8}$ and $P = 5 \times 10^{-9}$ and from all five loci with P values ranging from $P = 1 \times 10^{-6}$ to $P = 5 \times 10^{-8}$ (Online Methods) for genotyping in an additional 7,170 European individuals in order to boost the study's power. In a joint analysis combining all 47,577 individuals, the significance for the four loci with P values between $P = 5 \times 10^{-8}$ and $P = 5 \times 10^{-9}$ increased, indicating these represent true positive associations (**Table 1**). The joint analysis also provided further evidence for two other loci (locus 21 near *DKK1* and locus 22 tagged by an intronic SNP in *GOSR2*) that reached genome-wide significance, bringing the total number of significant loci to 22, with 25 independently associated index SNPs (**Table 1**). The index SNP (rs1733724) in *DKK1* was previously associated with QRS duration in an Icelandic population[9].

Association with conduction defect

Based on this series of QRS associations, we sought to test the hypothesis that QRS-prolonging alleles, on average, increase risk of ventricular conduction defects. To address this question, we calculated a risk score in each individual by adding up the number of QRS-prolonging alleles identified in this study weighted by the observed effect sizes (β estimates) from the final meta-analysis. In an independent set of 519 individuals from the Atherosclerosis Risk in Communities (ARIC) and Rotterdam (RS) studies with bundle branch block or nonspecific prolongation of QRS interval (QRS > 120 milliseconds (ms)) compared with those individuals with normal conduction ($N = 12,804$), we found evidence that the cumulative burden of QRS-prolonging alleles is associated with risk of ventricular conduction defect ($P = 0.004$). This result was largely driven by those individuals with nonspecific

Table 1 Significant loci at $P < 5 \times 10^{-8}$ in combined GWAS and candidate SNP meta-analysis

Locus	Chr.	Index SNP	Coded/ non-coded Allele	AF	GWAS β	GWAS s.e.$_{GC}$	GWAS P_{GC}	I^2	PREVEND β	PREVEND P	$P_{Overall}$	Multi-SNP β	Multi-SNP P	Nearest gene	SNP annotation
1	3	rs6801957	T/C	0.41	0.77	0.07	1.10×10^{-28}	45.3	—	—	$\mathbf{1.10 \times 10^{-28}}$	0.54	$\mathbf{3.43 \times 10^{-14}}$	SCN10A	Intron
	3	rs9851724	C/T	0.33	−0.66	0.07	1.91×10^{-20}	57.1	—	—	$\mathbf{1.91 \times 10^{-20}}$	−0.60	$\mathbf{5.78 \times 10^{-16}}$	SCN10A-SCN5A	Intergenic
	3	rs10865879	T/C	0.41	0.77	0.07	1.10×10^{-28}	53.6	—	—	$\mathbf{1.10 \times 10^{-28}}$	0.33	1.67×10^{-4}	SCN5A/EXOG	Intergenic
	3	rs11710077	T/A	0.21	−0.84	0.09	5.74×10^{-22}	23.8	—	—	$\mathbf{5.74 \times 10^{-22}}$	−0.44	$\mathbf{1.33 \times 10^{-6}}$	SCN5A	Intron
	3	rs11708996	C/G	0.16	0.79	0.10	1.26×10^{-16}	0.0	—	—	$\mathbf{1.26 \times 10^{-16}}$	0.47	$\mathbf{7.23 \times 10^{-6}}$	SCN5A	Intron
	3	rs2051211	G/A	0.26	−0.44	0.08	1.57×10^{-8}	0.0	—	—	$\mathbf{1.57 \times 10^{-8}}$	−0.18	3.71×10^{-2}	EXOG	Intron
2	6	rs9470361	A/G	0.25	0.87	0.08	3.00×10^{-27}	14.6	—	—	$\mathbf{3.00 \times 10^{-27}}$	—	—	CDKN1A	Intergenic
3	6	rs11153730	C/T	0.49	0.59	0.07	1.26×10^{-18}	5.3	—	—	$\mathbf{1.26 \times 10^{-18}}$	—	—	C6orf204-SLC35F1-PLN-BRD7P3	Intergenic
4	1	rs9436640	G/T	0.46	−0.59	0.07	4.57×10^{-18}	51.2	—	—	$\mathbf{4.57 \times 10^{-18}}$	—	—	NFIA	Intron
5	5	rs13165478	A/G	0.36	−0.55	0.07	7.36×10^{-14}	64.6	—	—	$\mathbf{7.36 \times 10^{-14}}$	—	—	HAND1-SAP30L	Intergenic
6	7	rs1362212	A/G	0.18	0.69	0.09	1.12×10^{-13}	0.0	—	—	$\mathbf{1.12 \times 10^{-13}}$	—	—	TBX20	Intergenic
7	14	rs11848785	G/A	0.27	−0.50	0.08	1.04×10^{-10}	0.0	—	—	$\mathbf{1.04 \times 10^{-10}}$	—	—	SIPA1L1	Intron
8	12	rs883079	C/T	0.29	0.49	0.08	1.33×10^{-10}	8.3	—	—	$\mathbf{1.33 \times 10^{-10}}$	—	—	TBX5	3′ UTR
9	12	rs10850409	A/G	0.27	−0.49	0.08	3.06×10^{-10}	0.0	—	—	$\mathbf{3.06 \times 10^{-10}}$	—	—	TBX3	Intergenic
10	10	rs7342028	T/G	0.27	0.48	0.08	4.95×10^{-10}	0.0	—	—	$\mathbf{4.95 \times 10^{-10}}$	—	—	VTI1A	Intron
11	18	rs991014	T/C	0.42	0.42	0.07	6.20×10^{-10}	0.0	—	—	$\mathbf{6.20 \times 10^{-10}}$	—	—	SETBP1	Intron
12	2	rs17020136	C/T	0.21	0.51	0.08	1.90×10^{-9}	0.0	—	—	$\mathbf{1.90 \times 10^{-9}}$	—	—	HEATR5B-STRN	Intron
13	3	rs4687718	A/G	0.14	−0.63	0.11	6.25×10^{-9}	0.0	—	—	$\mathbf{6.25 \times 10^{-9}}$	—	—	TKT-PRKCD-CACNA1D	Intron
14	2	rs7562790	G/T	0.40	0.39	0.07	8.22×10^{-9}	0.0	—	—	$\mathbf{8.22 \times 10^{-9}}$	—	—	CRIM1	Intron
15	1	rs17391905	G/T	0.05	−1.35	0.23	8.72×10^{-9}	4.0	−1.17	0.005	$\mathbf{3.26 \times 10^{-10}}$	—	—	C1orf185-RNF11-CDKN2C-FAF1	Intergenic
16	17	rs9912468	G/C	0.43	0.39	0.07	1.06×10^{-8}	28.2	—	—	$\mathbf{1.06 \times 10^{-8}}$	—	—	PRKCA	Intron
17	7	rs7784776	G/A	0.43	0.39	0.07	1.42×10^{-8}	0.0	0.36	0.015	$\mathbf{1.28 \times 10^{-9}}$	—	—	IGFBP3	Intergenic
18	1	rs4074536	C/T	0.29	−0.42	0.07	2.36×10^{-8}	0.5	—	—	$\mathbf{2.36 \times 10^{-8}}$	—	—	CASQ2	Missense
19	13	rs1886512	A/T	0.37	−0.40	0.07	4.31×10^{-8}	0.0	−0.28	0.047	$\mathbf{1.27 \times 10^{-8}}$	—	—	KLF12	Intron
20	3	rs2242285	A/G	0.42	0.37	0.07	4.79×10^{-8}	35.4	0.29	0.040	$\mathbf{1.09 \times 10^{-8}}$	—	—	LRIG1-SLC25A26	Intron
21	10	rs1733724	A/G	0.25	0.49	0.09	1.26×10^{-7}	0.0	0.34	0.035	$\mathbf{3.05 \times 10^{-8}}$	—	—	DKK1	Intergenic
22	17	rs17608766	C/T	0.16	0.53	0.10	3.71×10^{-7}	13.8	0.92	4.7×10^{-5}	$\mathbf{4.75 \times 10^{-10}}$	—	—	GOSR2	Intron, 3′ UTR

In each locus, at least one marker exceeded the genome-wide significance threshold of $P < 5 \times 10^{-8}$. At locus 1, six signals were identified ($r^2 < 0.05$) that exceeded this genome-wide threshold. In a multi-SNP model that included all six SNPs, there was evidence that at least four of these SNPs were independently associated with QRS duration.
The bolded allele is the coded allele. β values estimate the difference in QRS interval in milliseconds per copy of the coded allele, adjusted for the covariates in the model.
Chr., chromosome; AF, coded allele frequency; s.e., standard error; GC, genomic-control adjusted; UTR, untranslated region. AF is an average weighted by study size.

intraventricular conduction defects, as opposed to those with left or right bundle branch block (**Supplementary Table 3a,b**). Similar results were observed using an unweighted genotype risk score.

Putative functional variants

Of the 612 genome-wide significant SNPs, one in *SCN5A* (rs1805124, His558Arg, $P = 2.4 \times 10^{-18}$), two in *SCN10A* (rs12632942, Leu1092Pro, $P = 5.1 \times 10^{-11}$, and rs6795970, Ala1073Val, $P = 5 \times 10^{-27}$), one in *C6orf204* near *PLN* (rs3734381, Ser137Gly, $P = 1.1 \times 10^{-10}$) and one in *CASQ2* (index SNP rs4074536, Thr66Ala, $P = 2.4 \times 10^{-8}$) were non-synonymous (**Fig. 2** and **Supplementary Fig. 2**). The PolyPhen-2 program predicts all five of these variants to be benign, which is consistent with small-effect associations: each copy of the minor allele was associated with cross-sectional differences in QRS duration of less than 1 ms.

The 25 index SNPs (**Table 1**) were subsequently tested for association with gene *cis* expression levels in 1,240 PAXgene whole blood samples[10]. Four *cis* expression QTLs (eQTLs) were detected after stringent Bonferroni correction (**Supplementary Fig. 3**). The most notable eQTLs were observed for probes in exonic regions of *TKT* (rs4687718, $P = 5.87 \times 10^{-70}$) and *CDKN1A* (rs9470361, $P = 1.41 \times 10^{-10}$) and in an intronic probe for *C6orf204* near *PLN* (rs11153730,

$P = 1.54 \times 10^{-10}$). We additionally assessed *cis* regulation for all HapMap SNPs for these three loci (± 250 kb around the SNPs). The top eSNPs for *TKT* (rs9821134) and *C6orf204* (rs11970286) were in moderate to high LD ($r^2 = 0.47$ and $r^2 = 0.91$, respectively) with the top QRS signals at these loci. However, the top eSNP for *CDKN1A*, rs735013, was only weakly correlated with the QRS index SNP rs9470361 ($r^2 = 0.089$). In a conditional analysis that included both *CDKN1A* locus SNPs in the regression model, both rs735013 and rs9470361 remained independently associated with expression levels ($P = 1.7 \times 10^{-9}$ and $P = 2.3 \times 10^{-5}$, respectively). Additionally, rs735013 itself was marginally associated with QRS duration (coded allele frequency = 0.39, $\beta = 0.33$ ms (s.e. = 0.07 ms), $P = 2.4 \times 10^{-6}$). Whether these associations in whole blood samples will be similar to associations in cardiac myocytes and conduction tissue deserves further investigation.

Pleiotropic effects of ECG-associated variants

To explore the shared genetic underpinnings between atrial and ventricular depolarization and conduction (as measured by PR and QRS intervals) as well as ventricular depolarization and repolarization (QRS and QT intervals), we examined the effects of previously published PR and QT SNPs with respect to QRS interval. Several QRS loci were

Figure 2 Association plots for select loci. Each SNP is plotted with respect to its chromosomal location (x axis) and its *P* value (*y* axis on the left). The tall blue spikes indicate the recombination rate (*y* axis on the right) at that region of the chromosome. The blue-outlined triangles indicate coding region SNPs. (**a**) Locus 1 (*SCN5A-SCN10A)* on chromosome 3. The six index signals are named with their rs numbers and highlighted in different colors (yellow, green, teal, blue, purple and red). Other SNPs in linkage disequilibrium with the index SNP are denoted in the same color. Color saturation indicates the degree of correlation with the index SNP. (**b**) Locus 8 (*TBX5*) and locus 9 (*TBX3*) on chromosome 12. (**c**) Locus 12 (*HEATR5B-STRN*) and locus 14 (*CRIM1*) on chromosome 2.

previously associated with PR or QT intervals, including *PLN*, *TBX5-TBX3* and *SCN5A-SCN10A*, the last of which is associated with all three traits (**Supplementary Table 4a**). We also tested 9 PR SNPs and 16 QT SNPs for their effect on QRS duration (**Supplementary Table 4b**)[11–13]. Our results suggest roles for *CAV1-CAV2* (rs3807989, $P = 5.8 \times 10^{-6}$) and *NOS1AP* (rs12143842, $P = 1.3 \times 10^{-4}$) in QRS duration. Indeed *CAV1-CAV2* was recently associated with QRS interval[9].

QRS duration is positively correlated with both PR interval ($r = 0.09$) and QT interval ($r = 0.44$)[9]. To test if these relationships are also observed genetically, we compared the directionality of the association of SNPs at the published PR and QT loci with those for QRS duration. Generally, the effects of SNPs on PR interval were positively correlated with their effects on QRS duration ($r = 0.53$). With the exception of *TBX3*, the loci influencing both PR and QRS intervals (*SCN5A*, *SCN10A*, *TBX5* and *CAV1-CAV2*) do so in a concordant fashion (that is, variants that prolong PR also prolong QRS duration) (**Fig. 3** and **Supplementary Table 4a,b**). By contrast, although QT and QRS are positively correlated at the population level, the effects of SNPs on QT interval were marginally negatively correlated with their effects on QRS interval ($r = -0.08$). Of the index SNPs at the four loci significantly associated with both QT and QRS interval (*SCN5A-SCN10A*, *PRKCA*, *NOS1AP* and *PLN*), only the *PLN* locus SNPs showed effects in the same direction (**Fig. 3** and **Supplementary Table 4a,b**).

Bioinformatic network analysis of QRS-associated loci
To examine the relationships between genetic loci associated with QRS duration, we developed an *in silico* relational network linking the loci based on published direct gene product interactions obtained from curated databases (**Supplementary Fig. 4**)[14]. Most loci meeting genome-wide significance mapped to this network after a minimum number of 'linker' nodes were incorporated to create a spanning
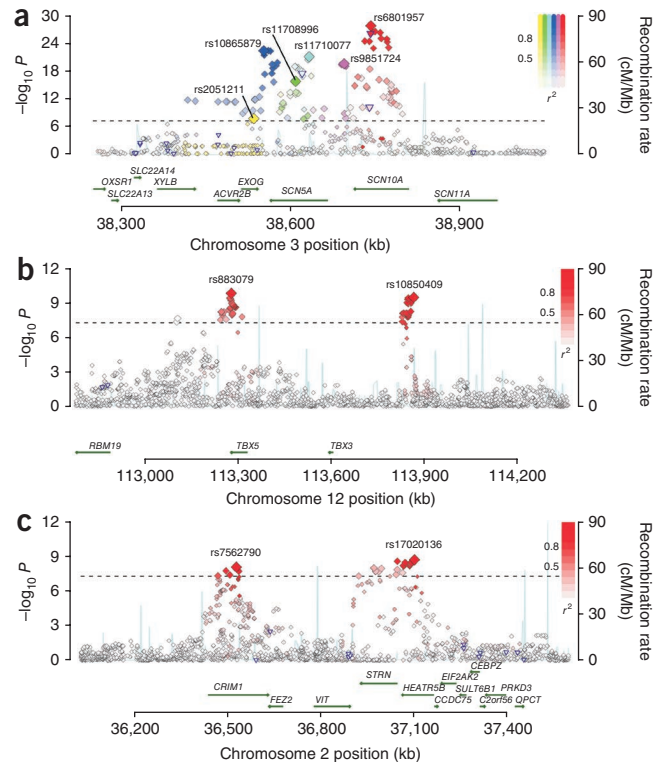
network. This analysis provides a graphical overview of the interconnections among QRS-associated genetic loci and highlights both known and putative molecular mechanisms regulating ventricular conduction (see below for further discussion). Several of the 'linker' nodes incorporated in the network, such as *GJA1* (encoding connexin 43), *NEDD4*, *KCNMA1* and *RYR2*, are known modulators of cardiac electrical activity. Functional enrichment analysis of the QRS-associated network nodes (that is, loci with $P < 5 \times 10^{-8}$) using two independent software tools revealed that programs involved in heart development were highly overrepresented (*P* value range: $P = 5.8 \times 10^{-6}$ to $P = 9.6 \times 10^{-5}$)[15,16].

SCN10A function in a mouse model
We undertook functional studies to determine whether our most significant locus was associated with ventricular conduction in mice. Transcriptional profiling suggests that *Scn10a* mRNA, which encodes the $Na_v1.8$ sodium channel, is expressed in the ventricular myocardium and at higher levels in the specialized conduction system[17]. These data were confirmed and extended by quantitative
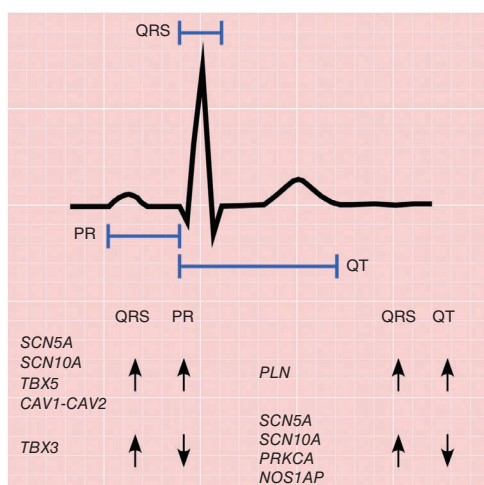

Figure 3 Pleiotropic associations of PR, QRS and QT loci. Electrocardiographic tracing delineating the PR, QRS and QT intervals. PR and QRS intervals reflect myocardial depolarization and conduction time through the atria and down the atrioventricular node (PR) and throughout the ventricle (QRS) and are weakly positively correlated ($r = 0.09$). The majority of loci that influence both PR and QRS (*SCN5A*, *SCN10A*, *TBX5* and *CAV1-2)* do so in a concordant fashion (meaning variants that prolong PR duration also prolong QRS duration). The notable exception is a region on chromosome 12, where variants in the *TBX5* locus have a concordant effect, whereas those in nearby *TBX3* have a discordant effect. By contrast, although QRS (ventricular depolarization) and QT (ventricular repolarization) are moderately positively correlated, the majority of loci (*SCN5A*, *SCN10A*, *PRKCA* and *NOS1AP)* that influence both phenotypes do so in a discordant fashion (meaning variants that prolong the QRS interval shorten the QT interval). The exception is the locus at *PLN*, where the variants have a concordant effect.

Figure 4 Expression and function of Scn10a in the mouse heart. (**a**) Neonatal ventricular myocytes from *Cntn2-eGFP* BAC transgenic mice were fluorescence-activated cell sorted and eGFP+ and eGFP− pools were analyzed by RT-PCR. Transcripts encoding eGFP, Cntn2 and Scn10a were highly enriched in the eGFP+ fraction. Quantitative RT-PCR demonstrated 25.7-fold enrichment of *Scn10a* Na$_v$1.8. (**b**) Representative telemetric electrocardiographic recordings (lead II configuration) obtained 30 min after administration of vehicle alone (black tracing) or the *Scn10a* Na$_v$1.8 antagonist A-803467 (green tracing). The two tracings are aligned at the onset of the QRS wave, and both PR interval and QRS interval prolongation were observed in drug-treated mice. (**c**) Representative intracardiac recordings showing HV intervals obtained before (Pre) and after (Post) administration of vehicle or A-803467. Significant HV prolongation was observed in drug-treated mice.
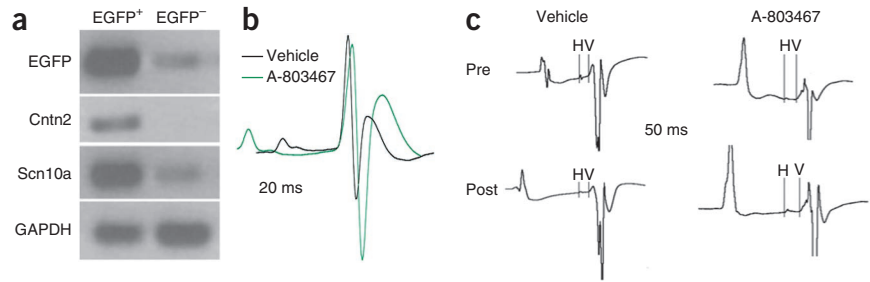
PCR (**Fig. 4a**), demonstrating a 25.7-fold ± 1.1-fold (s.e.) enrichment of *Scn10a* Na$_v$1.8 in Purkinje cells compared to working ventricular myocytes (*n* = 3 for each cell type; *P* = 0.002).

Telemetric electrocardiographic recordings (lead II position) were obtained in conscious mice treated with A-803467, a potent *Scn10a* Na$_v$1.8 antagonist, which blocks Na$_v$1.8 100 times more potently than Na$_v$1.5 with the doses used[18]. These studies showed a significant increase in QRS duration (11.6 ms (± 2.6 ms (s.e.)) to 14.5 ms (± 0.54 ms), *n* = 7, *P* < 0.001), whereas treatment with vehicle alone was without effect (11.4 ms (± 0.29 ms) to 11.9 ms (± 0.42 ms), *n* = 7, *P* value was not significant). The PR interval was also increased in drug-treated mice, from 31.4 ms (± 0.98 ms) to 42.5 ms (± 3.3 ms), *n* = 7, *P* < 0.01), whereas treatment with vehicle alone resulted in no significant change (32.6 ms (± 1.0 ms) to 33.4 ms (± 0.69 ms), *n* = 7, *P* value was not significant) (**Fig. 4b**). To further delineate the site of ventricular conduction slowing, we performed intra-cardiac recordings from mice treated with A-803467. These studies confirmed the significant increase in QRS duration (from 12.26 ms (± 0.62 ms) to 14.56 ms (± 0.58 ms), *n* = 7, *P* = 0.015), whereas treatment with vehicle alone was without significant effect (12.39 ms (± 0.52 ms) to 13.65 ms (± 0.97 ms), *n* = 5, *P* value was not significant). A-803467 treatment resulted in a 35.7% ± 1.2% increase in HV interval (from 9.33 ms (± 0.74 ms) to 12.67 ms (± 1.06 ms), *P* = 0.009), whereas treatment with vehicle alone was without significant effect (10.67 ms (± 0.83 ms) to 11.17 ms (± 1.10 ms, *P* value was not significant) (**Fig. 4c**). Taken together, these data indicate that the QRS prolongation may primarily reflect conduction slowing in the specialized ventricular conduction system.

DISCUSSION

Our meta-analysis of 14 GWAS consisting of 40,407 individuals of European descent with additional genotyping in 7,170 Europeans yielded genome-wide significant associations of QRS duration with common variants in 22 loci. Variations in four of these loci (locus 1, *SCN5A-SCN10A*; locus 2, *CDKN1A;* locus 8, *TBX5;* and locus 21, *DKK1*) were previously associated with QRS duration in smaller independent studies using both candidate gene and genome-wide approaches[7–9]. The 22 loci include genes in a number of interconnected pathways, including some previously known to be involved in cardiac conduction, such as sodium channels, calcium-handling proteins and transcription factors, as well as previously unidentified processes not known to be involved in cardiac electrophysiology, such as kinase inhibitors, growth factor-related genes and others.

The electrocardiographic QRS interval reflects ventricular depolarization and conduction time. Ventricular myocyte depolarization occurs through cardiac membrane excitatory inward currents mediated by voltage-gated sodium channels[19]. The primary determinants of conduction velocity are the magnitude of excitatory inward currents flowing through these sodium channels, the extent of cell-to-cell communication through gap junction–connexin coupling, and cell and tissue architecture and morphology[19]. Multiple pathways suggested in this study determine or modulate these key components of ventricular depolarization and conduction. Candidate genes in these pathways are briefly discussed in **Box 1**.

Our strongest association signal (locus 1) mapped in or near two voltage-gated sodium channel genes: *SCN5A* and *SCN10A*. *SCN5A* encodes the cardiac Na$_v$1.5 sodium channel and is well known for its role in cardiac conduction and other cardiovascular and electrophysiologic phenotypes[20,21]. *SCN10A* encodes the Na$_v$1.8 sodium channel. We provide new data demonstrating that the *SCN10A* transcript and product is preferentially expressed in the mouse His-Purkinje system compared with the ventricular myocardium, and that Na$_v$1.8 channel blockers result in QRS and HV interval prolongation, indicative of a slowing of impulse propagation in the specialized ventricular conduction system and a delayed activation of the ventricular myocardium. Notably, a recent study reported shortening of the PR interval in Scn10a knockdown mice and concluded that Na$_v$1.8 prolongs cardiac conduction and that rs6795970, encoding the A1073V variant, is a gain-of-function allele[8]. Alternatively, the more rapid conduction they observed in the knockdown mice could reflect compensatory upregulation of TTX-sensitive currents, a phenomenon previously observed in Na$_v$1.8-deficient DRG neurons[22].

We and others demonstrated previously that, in addition to their association with QRS duration, variants in *SCN5A* and *SCN10A* are associated with atrial conduction (PR interval) and myocardial repolarization (QT interval), as well as atrial and ventricular fibrillation[8,9,13]. These results emphasize the crucial role played by these genes in cardiac conduction and the generation of arrhythmias.

Calcium regulation is integral to impulse propagation, modulating cellular electrophysiology, including sodium channel and gap-junction function, as well as tissue architecture[20,23,24]. Several of the loci associated with QRS duration contain genes directly related to calcium processes. As depicted in **Supplementary Figure 4** and detailed in **Box 1**, these genes encode interrelated proteins that influence Ca^{2+} signaling (*PLN* in locus 3*; PRKCA* in locus 16; and *CASQ2* in locus 18) and downstream effects (*STRN* in locus 12).

Transcription factors regulating embryonic electrophysiologic development are critical for the integrity of impulse conduction[25]. We identified six transcription factors (*TBX3* in locus 9; *TBX5* in locus 8; *TBX20* in locus 6; *HAND1* in locus 5; *NFIA* in locus 4; and *KLF12* in locus 19) in loci associated with QRS duration. Several of these transcription factors affect cardiac morphogenesis and may influence conduction by altering cellular and tissue architecture. Notably, they may also have direct electrophysiologic consequences by modifying factors involved in impulse conduction. For example, *HAND1* and

T-box factors regulate *GJA5* (encoding connexin 40) and/or *GJA1* (encoding connexin 43), and *TBX5* binds to the *ATP2A2* (also known as *SERCA2A*) promoter[26].

Our study suggests a number of processes and pathways not previously known to be involved in cardiac electrophysiology, including cyclin-dependent kinase inhibitors and genes related to tumorigenesis

and cellular transformation. How these previously unidentified processes influence QRS duration remains to be defined.

In pleiotropic analyses, most variants influencing both PR and QRS interval, with the exception of *TBX3*, were concordant in effect direction, consistent with the known shared physiologic processes underlying the two traits: depolarization and conduction time in the sino-atrial node,

---

Box 1 Noteworthy genes within loci associated with QRS duration

Of the 22 loci identified, common variants in four loci (*SCN5A-SCN10A, CDKN1A, TBX5* and *DKK1*) were previously associated with QRS duration in genetic association studies. Mutations in two loci (*SCN5A* and *TBX5*) lead to inherited syndromes associated with conduction disease. Animal experiments show a role for several additional loci (*HAND1, TBX3* and *TBX5*) in cardiac ventricular conduction, as detailed below. The remainder are new QRS loci, and their role in cardiac conduction remains to be elucidated.

(1) Cardiac sodium channel genes:
- ***SCN5A* (locus 1):** *SCN5A* encodes the cardiac Na$_v$1.5 sodium channel and is well known to influence cardiac conduction, as well as other cardiovascular and electrophysiologic phenotypes[20,21].
- ***SCN10A* (locus 1):** *SCN10A* encodes the Na$_v$1.8 sodium channel, present in both ventricular myocardium and conduction fibers. Selective *SCN10A* blocker prolongs QRS interval.

(2) Calcium-handling proteins:
- ***CASQ2* (locus 18):** *CASQ2* regulates opening of the ryanodine receptor (encoded by *RYR2*)[28,29]. Cellular depolarization through sodium channels triggers calcium influx through L-type calcium channels, which in turn provokes *RYR2*-mediated calcium release from the sarcoplasmic reticulum. *CASQ2* mutations have been associated with catecholaminergic polymorphic ventricular tachycardia[30,31].
- ***PLN* (locus 3):** Calcium uptake into the sarcoplasmic reticulum by SERCA2a is regulated by *PLN* (encoding cardiac phospholamban)[32]. The phosphorylation state of *PLN* is dependent on signaling pathways involving phosphatases and kinases, including that encoded by *PRKCA*[41]. We previously demonstrated that this locus is associated with both cardiac electrical properties (QT interval duration and heart rate) and size (left ventricular end diastolic dimension) in genome-wide association analyses[11,12,33,34].
- ***PRKCA* (locus 16):** Protein kinase C alpha activity affects dephosphorylation of the sarcoplasmic reticulum Ca^{2+} ATPase-2 (SERCA-2) pump inhibitory protein phospholamban (PLN) and alters sarcoplasmic reticulum Ca^{2+} loading and the Ca^{2+} transient[35].
- ***STRN* (locus 12):** Striatin is a Ca^{2+}-calmodulin binding protein that directly binds to caveolin scaffolding protein. Striatin has recently been implicated in a canine model of arrhythmogenic right ventricular cardiomyopathy[36,37].

(3) Transcription factors:
- ***TBX3* (locus 9) and *TBX5* (locus 8):** *TBX3* and *TBX5* encode transcription factors found in the cardiac conduction system. *TBX5* (activator) competes with *TBX3* (repressor) for the regulation of working myocardial genes such as *GJA1*[38,39]. Common variations near *TBX3* and *TBX5* were associated with PR and QRS durations[9,13]. Mutations in *TBX3* and *TBX5* have been associated with rare inherited syndromes manifested by an array of defects including ventricular structural and/or conduction defects.
- ***TBX20* (locus 6):** *TBX20* demarcates the left and right ventricles[40] and mutations in *TBX20* have been implicated in multiple structural defects in mouse and human models[41,42].
- ***HAND1* (locus 5):** *HAND1* encodes a transcription factor essential to cardiac morphogenesis[43], with a mutation in this gene having been identified in human hearts with septal defects[44]. Overexpression of Hand1 in the adult mouse heart leads to loss of connexin 43 (encoded by *GJA1*) expression, QRS prolongation and predisposition to ventricular arrhythmia[45].
- ***NFIA* (locus 4) and *KLF12* (locus 19):** Little is known about the role of Nuclear Factor One (NFIA) and Kruppel like protein 12 (KLF12) in cardiac tissue development.

(4) Cyclin dependent kinase inhibitors:
- ***CDKN1A* (locus 2):** *CDKN1A* is a negative regulator of cell cycle entry into G2/M phase and is upregulated by *ERBB2* activation. *ERBB2,* encoding a member of the EGF-receptor family of tyrosine kinases, is essential for proper heart development, and its ligand neuregulin-1 promotes formation of the murine cardiac conduction system[46]. Furthermore, *ERBB2* can modulate gap junction assembly and alter appropriate phosphorylation of connexin 43 in glial cells[47]. In addition, *CDKN1A* is upregulated by *PRKCA* (locus 16)[48].
- ***CDKN2C* (locus 15):** A member of the family of cyclin-dependent kinase inhibitors that prevent the activation of the CDK kinases, thus functioning as a cell-growth regulator that controls cell cycle G1 progression.

(5) Other pathways:
- ***CRIM1* (locus 14):** *CRIM1*, encoding a cell-surface transmembrane protein that may bind to various members of the TGF-beta superfamily of ligands, is expressed in mouse and human cardiac tissues[49,50]. *CRIM1* interacts with bone morphogenetic proteins, which induce the expression of *CDKN1A* (p21)[49,51].
- ***LRIG1* (locus 20):** *LRIG1* is upregulated in malignancies. It negatively regulates the proto-oncogenic, tyrosine kinase receptor family ERBB2 (ref. 52).
- ***SETBP1* (locus 11):** *SETBP1* encodes a ubiquitously expressed protein that binds to *SET* (ref. 53). The *SETBP1-SET* interaction has been hypothesized to be a component in tumor development.
- ***TKT* (locus 13):** Transketolase (TKT) is a ubiquitous enzyme used in multiple metabolic pathways, including the pentose phosphate pathway[54].
- ***DKK1* (locus 21):** *DKK1*, implicated in several tumors, inhibits the Wnt signaling pathway[55]. Wnt signaling is an important modulator of connexin43-dependent intercellular coupling in the heart[56]. In cardiac tissue, it has an embryologic role with regard to axial development[57].
- ***SIPA1L1* (locus 7):** *SIPA1L1* appears to play a role in non-canonical Wnt signaling and contributes to development[58].

atria and atrioventricular node (PR interval) and depolarization and conduction time in the ventricles (QRS interval). By contrast, although QRS (ventricular depolarization) and QT (ventricular repolarization) are moderately positively correlated, most loci influencing both traits showed discordant effect directions (with the exception of the *PLN* locus). Investigating the physiologic foundations for these concordant and discordant PR-QRS and QT-QRS relationships could be particularly informative for elucidating the mechanisms by which these loci influence cardiac depolarization, conduction and repolarization.

Several limitations of our study should be considered. First, although we have identified 22 loci significantly associated with QRS duration, the broad nature of LD among common variants generally precludes an unambiguous identification of the culprit variant or of the functional gene. For several genes (*SCN5A*, *SCN10A*, *C6orf204* and *CASQ2*), there are common coding SNPs in high LD with the index SNP, which may lend some support for a functional role for these genes. Furthermore, our expression analysis in blood revealed very strong *cis*-eQTL associations for *TKT* and *CDKN1A*, lending additional support to these genes as functional candidates. It would be desirable to perform similar eQTL analyses based on expression data in myocardial cells or in conduction tissue. For our top signal in *SCN10A*, a gene which until recently was not known to be expressed in the heart, our functional work in mice confirms that *SCN10A* is involved in ventricular depolarization and conduction. Further fine mapping is needed at all 22 loci to conclusively test all genetic variation (rare and common) for a role in QRS modulation.

To minimize the potential for confounding due to population substructure, we limited our analyses to individuals of European descent, a population for which we could assemble the largest number of samples. At the individual study level, the GWAS showed very little evidence for gross stratification (genomic inflation factor, λ_{GC}, values ranged from 1.00 to 1.05). However, one of our QRS loci, mapping to *HAND1-SAP30L*, showed evidence of heterogeneity. In genetic association studies, heterogeneity can be due to sampling error, differences in phenotypic measurement, differences in LD structure between populations, technical artifacts, or genuine biological heterogeneity, but it would be difficult to conclude on the basis of our data here which of these is the most likely explanation[27].

Our study underscores the power of a large genome-wide association study to extend prior biological understanding of cardiac ventricular conduction. Better understanding of the complex biologic pathways and molecular genetics associated with cardiac conduction and QRS duration may offer insight into the molecular basis underlying the pathogenesis of conduction abnormalities that can result in increased risk of sudden death, heart failure and cardiac mortality.

URLs. MACH, http://www.sph.umich.edu/csg/abecasis/mach/; MANTEL, http://www.broadinstitute.org/~debakker/mantel.html; MetABEL, http://mga.bionet.nsc.ru/~yurii/ABEL/; BIMBAM, http://quartus.uchicago.edu/~yguan/bimbam/; METAL, http://www.sph.umich.edu/csg/abecasis/metal/; PLINK, http://pngu.mgh.harvard.edu/~purcell/plink/; IMPUTE, https://mathgen.stats.ox.ac.uk/impute/impute.html; SNPTEST, http://www.stats.ox.ac.uk/~marchini/software/gwas/snptest.html; 1000 Genomes Project, http:// www.1000Genomes.org/; SNAP, http://www.broadinstitute.org/mpg/snap/; Ingenuity, http://www.ingenuity.com/; DAVID, http://david.abcc.ncifcrf.gov/; GOTM, http://bioinfo.vanderbilt.edu/webgestalt/.

METHODS
Methods and any associated references are available in the online version of the paper at http://www.nature.com/naturegenetics/.

Note: Supplementary information is available on the Nature Genetics website.

1. Desai, A.D. *et al.* Prognostic significance of quantitative QRS duration. *Am. J. Med.* **119**, 600–606 (2006).
2. Elhendy, A., Hammill, S.C., Mahoney, D.W. & Pellikka, P.A. Relation of QRS duration on the surface 12-lead electrocardiogram with mortality in patients with known or suspected coronary artery disease. *Am. J. Cardiol.* **96**, 1082–1088 (2005).
3. Oikarinen, L. *et al.* QRS duration and QT interval predict mortality in hypertensive patients with left ventricular hypertrophy: the Losartan Intervention for Endpoint Reduction in Hypertension Study. *Hypertension* **43**, 1029–1034 (2004).
4. Dhingra, R. *et al.* Electrocardiographic QRS duration and the risk of congestive heart failure: the Framingham Heart Study. *Hypertension* **47**, 861–867 (2006).
5. Busjahn, A. *et al.* QT interval is linked to 2 long-QT syndrome loci in normal subjects. *Circulation* **99**, 3161–3164 (1999).
6. Hanson, B. *et al.* Genetic factors in the electrocardiogram and heart rate of twins reared apart and together. *Am. J. Cardiol.* **63**, 606–609 (1989).
7. Bezzina, C.R. *et al.* Common sodium channel promoter haplotype in Asian subjects underlies variability in cardiac conduction. *Circulation* **113**, 338–344 (2006).
8. Chambers, J.C. *et al.* Genetic variation in *SCN10A* influences cardiac conduction. *Nat. Genet.* **42**, 149–152 (2010).
9. Holm, H. *et al.* Several common variants modulate heart rate, PR interval and QRS duration. *Nat. Genet.* **42**, 117–122 (2010).
10. Dubois, P.C. *et al.* Multiple common variants for celiac disease influencing immune gene expression. *Nat. Genet.* **42**, 295–302 (2010).
11. Newton-Cheh, C. *et al.* Common variants at ten loci influence QT interval duration in the QTGEN Study. *Nat. Genet.* **41**, 399–406 (2009).
12. Pfeufer, A. *et al.* Common variants at ten loci modulate the QT interval duration in the QTSCD Study. *Nat. Genet.* **41**, 407–414 (2009).
13. Pfeufer, A. *et al.* Genome-wide association study of PR interval. *Nat. Genet.* **42**, 153–159 (2010).
14. Calvano, S.E. *et al.* A network-based analysis of systemic inflammation in humans. *Nature* **437**, 1032–1037 (2005).
15. Huang, W., Sherman, B.T. & Lempicki, R.A. Systematic and integrative analysis of large gene lists using DAVID bioinformatics resources. *Nat. Protoc.* **4**, 44–57 (2009).

16. Zhang, B., Schmoyer, D., Kirov, S. & Snoddy, J. GOTree Machine (GOTM): a web-based platform for interpreting sets of interesting genes using Gene Ontology hierarchies. *BMC Bioinformatics* **5**, 16 (2004).
17. Pallante, B.A. *et al.* Contactin-2 expression in the cardiac Purkinje fiber network. *Circ. Arrhythm. Electrophysiol.* **3**, 186–194 (2010).
18. Jarvis, M.F. *et al.* A-803467, a potent and selective Nav1.8 sodium channel blocker, attenuates neuropathic and inflammatory pain in the rat. *Proc. Natl. Acad. Sci. USA* **104**, 8520–8525 (2007).
19. Desplantez, T., Dupont, E., Severs, N.J. & Weingart, R. Gap junction channels and cardiac impulse propagation. *J. Membr. Biol.* **218**, 13–28 (2007).
20. Abriel, H. Cardiac sodium channel Na(v)1.5 and interacting proteins: physiology and pathophysiology. *J. Mol. Cell. Cardiol.* **48**, 2–11 (2010).
21. Remme, C.A., Wilde, A.A. & Bezzina, C.R. Cardiac sodium channel overlap syndromes: different faces of *SCN5A* mutations. *Trends Cardiovasc. Med.* **18**, 78–87 (2008).
22. Akopian, A.N. *et al.* The tetrodotoxin-resistant sodium channel SNS has a specialized function in pain pathways. *Nat. Neurosci.* **2**, 541–548 (1999).
23. Saimi, Y. & Kung, C. Calmodulin as an ion channel subunit. *Annu. Rev. Physiol.* **64**, 289–311 (2002).
24. Potet, F. *et al.* Functional interactions between distinct sodium channel cytoplasmic domains through the action of calmodulin. *J. Biol. Chem.* **284**, 8846–8854 (2009).
25. Wolf, C.M. & Berul, C.I. Inherited conduction system abnormalities—one group of diseases, many genes. *J. Cardiovasc. Electrophysiol.* **17**, 446–455 (2006).
26. Zhu, Y. *et al.* Tbx5-dependent pathway regulating diastolic function in congenital heart disease. *Proc. Natl. Acad. Sci. USA* **105**, 5519–5524 (2008).
27. Lebrec, J.J., Stijnen, T. & van Houwelingen, H.C. Dealing with heterogeneity between cohorts in genomewide SNP association studies. *Stat. Appl. Genet. Mol. Biol.* **9** article 8 (2010).
28. Wei, L., Hanna, A.D., Beard, N.A. & Dulhunty, A.F. Unique isoform-specific properties of calsequestrin in the heart and skeletal muscle. *Cell Calcium* **45**, 474–484 (2009).
29. Terentyev, D. *et al.* Abnormal interactions of calsequestrin with the ryanodine receptor calcium release channel complex linked to exercise-induced sudden cardiac death. *Circ. Res.* **98**, 1151–1158 (2006).
30. Priori, S.G. *et al.* Clinical and molecular characterization of patients with catecholaminergic polymorphic ventricular tachycardia. *Circulation* **106**, 69–74 (2002).
31. Postma, A.V. *et al.* Absence of calsequestrin 2 causes severe forms of catecholaminergic polymorphic ventricular tachycardia. *Circ. Res.* **91**, e21–e26 (2002).
32. Wang, Y. & Goldhaber, J.I. Return of calcium: manipulating intracellular calcium to prevent cardiac pathologies. *Proc. Natl. Acad. Sci. USA* **101**, 5697–5698 (2004).
33. Vasan, R.S. *et al.* Genetic variants associated with cardiac structure and function: a meta-analysis and replication of genome-wide association data. *J. Am. Med. Assoc.* **302**, 168–178 (2009).
34. Eijgelsheim, M. *et al.* Genome-wide association analysis identifies multiple loci related with resting heart rate. *Hum. Mol. Genet.* **19**, 3885–3895 (2010).
35. Braz, J.C. *et al.* PKC-alpha regulates cardiac contractility and propensity toward heart failure. *Nat. Med.* **10**, 248–254 (2004).
36. Baillat, G. *et al.* Molecular cloning and characterization of phocein, a protein found from the Golgi complex to dendritic spines. *Mol. Biol. Cell* **12**, 663–673 (2001).
37. Meurs, K.M. *et al.* Genome-wide association identifies a deletion in the 3′ untranslated region of Striatin in a canine model of arrhythmogenic right ventricular cardiomyopathy. *Hum. Genet.* **128**, 315–324. (2010).
38. Boogerd, K.J. *et al.* Msx1 and Msx2 are functional interacting partners of T-box factors in the regulation of Connexin43. *Cardiovasc. Res.* **78**, 485–493 (2008).
39. Hoogaars, W.M. *et al.* The transcriptional repressor Tbx3 delineates the developing central conduction system of the heart. *Cardiovasc. Res.* **62**, 489–499 (2004).
40. Singh, R. *et al.* Tbx20 interacts with smads to confine tbx2 expression to the atrioventricular canal. *Circ. Res.* **105**, 442–452 (2009).
41. Posch, M.G. *et al.* A gain-of-function *TBX20* mutation causes congenital atrial septal defects, patent foramen ovale and cardiac valve defects. *J. Med. Genet.* **47**, 230–235 (2009).
42. Bakker, M.L. *et al.* Transcription factor Tbx3 is required for the specification of the atrioventricular conduction system. *Circ. Res.* **102**, 1340–1349 (2008).
43. Riley, P., Anson-Cartwright, L. & Cross, J.C. The Hand1 bHLH transcription factor is essential for placentation and cardiac morphogenesis. *Nat. Genet.* **18**, 271–275 (1998).
44. Reamon-Buettner, S.M. *et al.* A functional genetic study identifies *HAND1* mutations in septation defects of the human heart. *Hum. Mol. Genet.* **18**, 3567–3578 (2009).
45. Breckenridge, R.A. *et al.* Overexpression of the transcription factor Hand1 causes predisposition towards arrhythmia in mice. *J. Mol. Cell. Cardiol.* **47**, 133–141 (2009).
46. Rentschler, S. *et al.* Neuregulin-1 promotes formation of the murine cardiac conduction system. *Proc. Natl. Acad. Sci. USA* **99**, 10464–10469 (2002).
47. Hofer, A. *et al.* C-erbB2/neu transfection induces gap junctional communication incompetence in glial cells. *J. Neurosci.* **16**, 4311–4321 (1996).
48. Besson, A. & Yong, V.W. Involvement of p21(Waf1/Cip1) in protein kinase C alpha-induced cell cycle progression. *Mol. Cell. Biol.* **20**, 4580–4590 (2000).
49. Wilkinson, L. *et al.* *CRIM1* regulates the rate of processing and delivery of bone morphogenetic proteins to the cell surface. *J. Biol. Chem.* **278**, 34181–34188 (2003).
50. Kolle, G., Georgas, K., Holmes, G.P., Little, M.H. & Yamada, T. *CRIM1*, a novel gene encoding a cysteine-rich repeat protein, is developmentally regulated and implicated in vertebrate CNS development and organogenesis. *Mech. Dev.* **90**, 181–193 (2000).
51. Pardali, K., Kowanetz, M., Heldin, C.H. & Moustakas, A. Smad pathway-specific transcriptional regulation of the cell cycle inhibitor p21(WAF1/Cip1). *J. Cell. Physiol.* **204**, 260–272 (2005).
52. Laederich, M.B. *et al.* The leucine-rich repeat protein LRIG1 is a negative regulator of ErbB family receptor tyrosine kinases. *J. Biol. Chem.* **279**, 47050–47056 (2004).
53. Minakuchi, M. *et al.* Identification and characterization of SEB, a novel protein that binds to the acute undifferentiated leukemia-associated protein SET. *Eur. J. Biochem.* **268**, 1340–1351 (2001).
54. Zhao, J. & Zhong, C.J. A review on research progress of transketolase. *Neurosci. Bull.* **25**, 94–99 (2009).
55. Fedi, P. *et al.* Isolation and biochemical characterization of the human Dkk-1 homologue, a novel inhibitor of mammalian Wnt signaling. *J. Biol. Chem.* **274**, 19465–19472 (1999).
56. Ai, Z., Fischer, A., Spray, D.C., Brown, A.M. & Fishman, G.I. Wnt-1 regulation of connexin43 in cardiac myocytes. *J. Clin. Invest.* **105**, 161–171 (2000).
57. Korol, O., Gupta, R.W. & Mercola, M. A novel activity of the Dickkopf-1 amino terminal domain promotes axial and heart development independently of canonical Wnt inhibition. *Dev. Biol.* **324**, 131–138 (2008).
58. Tsai, I.C. *et al.* A Wnt-CKIvarepsilon-Rap1 pathway regulates gastrulation by modulating SIPA1L1, a Rap GTPase activating protein. *Dev. Cell* **12**, 335–347 (2007).

[1]Division of Cardiology, Department of Medicine, University of Washington, Seattle, Washington, USA. [2]Cardiovascular Health Research Unit, Department of Medicine, University of Washington, Seattle, Washington, USA. [3]Genetic Epidemiology Unit, Department of Epidemiology, Erasmus Medical Center (MC), Rotterdam, The Netherlands. [4]Centre for Medical Systems Biology, Leiden, The Netherlands. [5]Division of Genetics, Department of Medicine, Brigham and Women's Hospital, Harvard Medical School, Boston, Massachusetts, USA. [6]Program in Medical and Population Genetics, Broad Institute, Cambridge, Massachusetts, USA. [7]Department of Medical Genetics, University Medical Center, Utrecht, The Netherlands. [8]Julius Center for Health Sciences and Primary Care, University Medical Center, Utrecht, The Netherlands. [9]Department of Internal Medicine B, Ernst Moritz Arndt University Greifswald, Greifswald, Germany. [10]Center for Human Genetic Research, Massachusetts General Hospital, Boston, Massachusetts, USA. [11]Cardiology Division, Massachusetts General Hospital, Boston, Massachusetts, USA. [12]National Heart, Lung, and Blood Institute's (NHLBI) Framingham Heart Study, Framingham, Massachusetts, USA. [13]Unit of Genetic Epidemiology and Bioinformatics, Department of Epidemiology, University Medical Center Groningen, University of Groningen, Groningen, The Netherlands. [14]Department of Cardiology, University Medical Center Groningen, University of Groningen, The Netherlands. [15]Institute of Medical Informatics, Biometry and Epidemiology, Chair of Epidemiology, Ludwig-Maximilians-Universität, Munich, Germany. [16]Department of Medicine I, University Hospital Grosshadern, Ludwig-Maximilians-Universität, Munich, Germany. [17]Institute of Epidemiology, Helmholtz Zentrum München-German Research Center for Environmental Health, Neuherberg, Germany. [18]Department of Epidemiology, Erasmus MC, Rotterdam, The Netherlands. [19]Division of Epidemiology and Community Health, School of Public Health, University of Minnesota, Minneapolis, Minnesota, USA. [20]Institute of Genetic Medicine, European Academy Bozen-Bolzano (EURAC), Bolzano, Italy, affiliated institute of the University of Lübeck, Germany. [21]Institute of Cardiovascular and Medical Sciences, College of Medical, Veterinary and Life Sciences, University of Glasgow, University Place, Glasgow, UK. [22]Medical Research Council (MRC) Human Genetics Unit, Institute of Genetics and Molecular Medicine, Edinburgh, UK. [23]Icelandic Heart Association, Kopavogur, Iceland. [24]University of Iceland, Reykjavik, Iceland. [25]Andrija Stampar School of Public Health, Medical School, University of Zagreb, Zagreb, Croatia. [26]Leon H. Charney Division of Cardiology, New York University School of Medicine, New York, New York, USA. [27]Department of Genetics, University Medical Center Groningen, University of Groningen, The Netherlands. [28]Section of Cardiovascular Medicine, Boston University School of Medicine, Boston, Massachusetts, USA. [29]Institute of Human Genetics, Helmholtz Zentrum München-German Research Center for Environmental Health, Neuherberg, Germany. [30]Institute of Human Genetics, Klinikum Rechts der Isar, Technische Universität München, Munich, Germany. [31]Center for Lung Biology, Department of Medicine, University of Washington, Seattle, Washington, USA. [32]Interfaculty Institute for Genetics and Functional Genomics, Ernst Moritz Arndt University Greifswald, Greifswald, Germany. [33]Department of Epidemiology and the Welch Center for Prevention, Epidemiology and Clinical Research, Johns Hopkins University, Baltimore, Maryland, USA. [34]Department of Internal Medicine, Erasmus MC, Rotterdam, The Netherlands. [35]Department of Epidemiology, Johns Hopkins University, Baltimore, Maryland, USA. [36]Clinical Pharmacology and Barts and the London Genome Centre, William Harvey Research Institute, Barts and the London School of Medicine, Queen Mary University of

London, London, UK. [37]Barts and the London National Institute of Health Research Cardiovascular Biomedical Research Unit, London, UK. [38]Department of Biostatistics, University of Washington, Seattle, Washington, USA. [39]Department of Biostatistics, Boston University School of Public Health, Boston, Massachusetts, USA. [40]Centre for Population Health Sciences, University of Edinburgh, Edinburgh, Scotland. [41]Department of Cardiology, Division of Heart and Lungs, University Medical Center Utrecht, Utrecht, The Netherlands. [42]McKusick-Nathans Institute of Genetic Medicine, Johns Hopkins University School of Medicine, Baltimore, Maryland, USA. [43]Department of Medical Informatics, Erasmus MC, Rotterdam, The Netherlands. [44]Institute of Clinical Chemistry and Laboratory Medicine, Ernst Moritz Arndt University Greifswald, Greifswald, Germany. [45]Laboratory of Epidemiology, Demography and Biometry, National Institute on Aging, National Institutes of Health, Bethesda, Maryland, USA. [46]Epidemiological Cardiology Research Center (EPICARE), Wake Forest University School of Medicine, Winston Salem, North Carolina, USA. [47]Department of Epidemiology, University of Washington, Seattle, Washington, USA. [48]Department of Health Services, University of Washington, Seattle, Washington, USA. [49]Group Health Research Institute, Group Health Cooperative, Seattle, Washington, USA. [50]Department of Clinical Genetics, Erasmus MC, Rotterdam, The Netherlands. [51]Institute for Biological and Medical Imaging, Helmholtz Zentrum München-German Research Center for Environmental Health, Neuherberg, Germany. [52]Netherlands Genomics Initiative (NGI)-sponsored Netherlands Consortium for Healthy Aging (NCHA), Rotterdam, The Netherlands. [53]Institute for Community Medicine, Ernst Moritz Arndt University Greifswald, Greifswald, Germany. [54]Department of Twin Research and Genetic Epidemiology Unit, St. Thomas' Campus, King's College London, St. Thomas' Hospital, London, UK. [55]Human Genetics Center, University of Texas Health Science Center at Houston, Houston, Texas, USA. [56]Institute for Molecular Medicine, University of Texas Health Science Center at Houston, Houston, Texas, USA. [57]Medical Genetics Institute, Cedars-Sinai Medical Center, Los Angeles, California, USA. [58]National Heart, Lung, and Blood Institute, Bethesda, Maryland, USA. [59]Klinikum Grosshadern, Munich, Germany. [60]Department of Pharmacology, Center for Pharmacology and Experimental Therapeutics, Ernst Moritz Arndt University Greifswald, Greifswald, Germany. [61]Department of Experimental and Diagnostic Medicine, University of Ferrara, Ferrara, Italy. [62]University of Dundee, Ninewells Hospital and Medical School, Dundee, UK. [63]Blizard Institute of Cell and Molecular Science, Barts and The London School of Medicine and Dentistry, Queen Mary University of London, London, UK. [64]Department of Pulmonology, University Medical Center Groningen, University of Groningen, Groningen, The Netherlands. [65]Department of Gastroenterology and Hepatology, University Medical Center Groningen, University of Groningen, Groningen, The Netherlands. [66]Department of Neurology, Rudolf Magnus Institute, University Medical Center Utrecht, University of Utrecht, Utrecht, The Netherlands. [67]Department of Medical Genetics and Rudolf Magnus Institute, University Medical Center Utrecht, Utrecht, The Netherlands. [68]Center for Neurobehavioral Genetics, University of California, Los Angeles, California, USA. [69]Department of Internal Medicine, University Medical Center Groningen, University of Groningen, Groningen, The Netherlands. [70]Centre for Global Health, Medical School, University of Split, Split, Croatia. [71]Gen-info Ltd. Zagreb, Croatia. [72]Department of Neurology, General Central Hospital, Bolzano, Italy. [73]Department of Neurology, University of Lübeck, Lübeck, Germany. [74]Division of Clinical Developmental Sciences, St. George's University of London, London, UK. [75]Inspectorate of Health Care, The Hague, The Netherlands. [76]Department of Cardiovascular Sciences, University of Leicester, Leicester, UK. [77]Leicester NIHR Biomedical Research Unit in Cardiovascular Disease Glenfield Hospital, Leicester, UK. [78]These authors contributed equally to this work. Correspondence should be addressed to N.S. (nsotoo@u.washington.edu), S.K. (skaab@med.lmu.de) or D.E.A. (arking@jhmi.edu).

ONLINE METHODS

Participating Studies. Details of the 15 participating studies are available in the **Supplementary Note**.

Phenotype modeling. We excluded individuals of non-European ancestry and those with QRS duration longer than 120 ms, which is often due to acquired left or right bundle branch block. We also excluded individuals with characteristics that may influence QRS duration, including a history of prior myocardial infarction or heart failure, atrial fibrillation on the electrocardiogram (ECG), pacemaker, Wolff-Parkinson-White syndrome, or use of class I and/or class III antiarrhythmic medications at the time of ECG acquisition. Covariates measured at baseline included age, gender, study site or cohort (if relevant), height and BMI.

GWAS genotyping and imputations. Either Affymetrix or Illumina arrays were used for genotyping (**Supplementary Table 1b**). Each study performed filtering of both individuals and SNPs to ensure robustness for genetic analysis (**Supplementary Table 1b**). Each study used the genotypes generated with these platforms to impute genotypes for approximately 2.5 million autosomal SNPs based on LD patterns observed in the HapMap European CEU samples. Imputed genotypes were coded as dosages, fractional values between 0 and 2 reflecting the estimated number of copies of a given allele for a given SNP for each individual. Most studies used a Hidden Markov model as implemented in the MACH software (see URLs). In the Cardiovascular Health Study (CHS) imputation was performed using BIMBAM (see URLs).

Extension genotyping. To extend our analyses, we genotyped nine SNP variants representing nine loci with P values ranging from $P = 1 \times 10^{-6}$ to $P = 5 \times 10^{-9}$ in an additional group of 7,170 individuals in the Prevention of Renal and Vascular Endstage (PREVEND) study. Of the nine SNPs, four represented loci with P values between $P = 5 \times 10^{-8}$ and $P = 5 \times 10^{-9}$ in the discovery phase (**Table 1**). The remaining five index SNPs (rs1733724 near *DKK1*; rs1662342 in an *MYL12A* intron; rs17608766, intronic in *GOSR2*; rs17362588, missense variant in *CCDC141*; rs2848901, intronic in *FHOD3*) had P values ranging from $P = 1 \times 10^{-6}$ to $P = 5 \times 10^{-8}$ and so needed additional statistical evidence in favor of the alternative hypothesis that they represented true associations. The SNPs were genotyped using TaqMan Allelic Discrimination Assays (ABI).

Statistical methods. Associations between QRS duration and SNPs were tested using linear regression models under the assumption of an additive (allelic trend, Armitage) model of genotypic effect. These models were adjusted for age, gender, height, BMI and study site (as appropriate). In family-based cohorts, linear mixed modeling was implemented to control for relatedness among samples[59]. A genomic control correction factor (λ_{GC}), calculated from all imputed SNPs, was applied on a per-study basis to account for cryptic population substructure and other potential biases[60].

The regression results were meta-analyzed using inverse variance weighted fixed-effects models[61]. We conducted the meta-analysis by using three independent analysts and three different software packages: MANTEL, MetABEL and METAL (see URLs). All the results were extremely concordant, reflecting a robust analysis. To be conservative, we subsequently corrected all P values from the meta-analysis for the overall inflation factor ($\lambda_{GC} = 1.059$). Results were considered statistically significant at a $P = 5 \times 10^{-8}$ after inflation correction, a figure that reflects the estimated testing burden of one million independent SNPs in samples of European ancestry[62]. Regions harboring association signals were visualized using SNAP[63].

To discern independent SNPs in regions with multiple genome-wide significant hits, we used an LD-binning procedure as implemented in PLINK. Starting with the most significant result as the index SNP, all surrounding SNPs within 500 kb (regardless of P value) with a very liberal pairwise $r^2 > 0.05$ were 'clumped' with the index SNP using LD patterns from HapMap CEU (release 27). The procedure was repeated until all SNPs found membership in a clump. Thus, all index SNPs are, by definition, in very weak LD (if at all) with one another (pairwise $r^2 < 0.05$) and are, as such, suggestive of independent signals of association.

We then evaluated a multivariate regression model based on 28 index SNPs that reached genome-wide significance in the discovery meta-analysis to test

which index SNPs represented true independent signals. We set the significance threshold for claiming independence based on the estimated number of uncorrelated tests we performed across the 20 genetic loci (that contain the 28 'independent' index SNPs). At these 20 loci, there are 21,551 SNPs surrounding the index SNPs within 500 kb in HapMap CEU samples, but after correcting for LD, we arrived at ~1,563 tests, which corresponds to a threshold of $P < 3.2 \times 10^{-5}$. Through meta-analysis of the multivariate P values across the participating cohorts with the largest sample sizes, we found significant evidence for four independent SNPs at the *SCN10A-SCN5A* locus (**Table 1**) but not elsewhere.

To test for an association with QRS greater than 120 ms, we calculated a SNP score for each individual in the RS and ARIC studies by adding up the number of QRS-prolonging alleles from the dosage counts and weighting by the β estimate from the meta-analysis. Logistic regression modeling was then performed with QRS greater than 120 ms as the dependent variable (dichotomous trait), which was regressed on the score, adjusting for age, sex, height, BMI and study site.

Because QRS interval is strongly influenced by sex, and inherited conduction defects can show a pronounced influence with aging, we explored whether the 23 genetic associations identified by our discovery GWAS meta-analysis (index SNPs at each of the 20 QRS-associated loci plus three additional independent SNPs at locus 1) differed by sex or age. For interactions with sex, we performed analyses in each cohort including an interaction term for sex × genotype, and then we used inverse variance weighting to meta-analyze the interaction terms. For interactions with age, each cohort performed separate analyses for each SNP stratified by decade, and then we performed regression analyses to assess the effect of age on the magnitude of the genetic effect.

eQTL analysis. We used genomics data from 1,240 PAXgene whole blood samples[10]. The samples were expression profiled on an Illumina HT-12 platform and genotyped using either an Illumina Hap370 or 610-Quad platform. Ungenotyped SNPs were imputed with the IMPUTE software (see URLs). We applied a 500-kb window (250 kb on each side) around each of the 25 QRS-associated SNPs and tested the *cis* expression-genotype association using SNPTEST (see URLs).

One hundred forty-two independent probes were examined at 22 QRS loci (comprising 25 index SNPs), resulting in a total of 198 probe-SNP pairs tested. Bonferroni adjustment was applied for the tested probe-SNP pairs ($P < 2.5 \times 10^{-4}$ was deemed significant). The eQTLs were checked for possible polymorphisms within the probe region. 1000 Genomes Project data (April 2009 release) was used to assess LD between the detected eSNP and the SNPs located within the probe region. If $r^2 > 0.05$ between an eSNP and the SNPs in the probe region, the eQTL was deemed a false positive assuming the 'probe SNP' caused differential hybridization.

Bioinformatics. All identified QRS loci were chosen to generate a gene product interaction network using Ingenuity Pathway Analysis software[14]. For locus 1, two genes were independently associated with QRS duration (*SCN5A-SCN10A*) and both were included in the network. For loci 3, 5, 12, 13, 15, 21 or 22, where it was difficult to discern to which of several genes the association signal might map, several genes (listed in **Table 1** for each of the loci) were included in the model. Of these seven loci, three (loci 13, 15 and 21) had two members each map to the network. We limited the relational network to known direct relationships (for example, protein-protein interaction, phosphorylation or physical binding). To ensure a spanning network, Ingenuity algorithmically incorporated additional nodes that interact with the QRS-associated loci. However, we limited these 'linkers' such that the relational distance among the QRS-associated loci was no more than one linker node. In some cases, this resulted in a genome-wide significant locus to remain unconnected to the network (for example, *GOSR2*, *CRIM1* and *NFIA*). We systematically searched PubMed to find direct gene product relationships among the network nodes to complement the original network. Relationships highlighted in this network have been compiled from a range of experimental conditions, organisms and tissue types, and therefore may not correspond to actual pathways in the human heart. For the functional enrichment analysis, we used two independent online tools, the Database for Annotation, Visualization and Integrated Discovery (DAVID, v6.7) and GOTree Machine (GOTM), to

identify Gene Ontology categories overrepresented among the QRS-associated loci relative to the entire human genome background[15,16]. A modified version of Fisher's Exact test (DAVID) and the hypergeometric test (GOTM) were used to determine the probability that a functional category is enriched compared to that expected from random chance.

Mouse model. *Quantitative real-time PCR.* Enhanced green fluorescent protein (EGFP)$^+$ Purkinje cells and EGFP$^-$ ventricular myocytes were isolated from neonatal *Cntn2-EGFP* transgenic mice by fluorescence-activated cell sorting[17,64]. Quantitative PCR was performed user primers (**Supplementary Table 5**) for SCN10A and ribosomal S26 as an internal reference using the 2-$\Delta\Delta$CT method[65].

Electrophysiologic testing. Telemetric devices (DSI) were implanted into adult CD1/129SI/SV1MJ mice and recordings were obtained before and 30 min after intraperitoneal injection of the Na$_v$1.8 antagonist A-803467 (100 mg/kg)[66]. Intracardiac recordings were obtained using an open-chest model under isoflurane anesthesia (1.5% v/v) using an octapolar catheter (EPR-800, Millar Instruments) placed in the right jugular vein.

59. Chen, W.M. & Abecasis, G.R. Family-based association tests for genomewide association scans. *Am. J. Hum. Genet.* **81**, 913–926 (2007).
60. Devlin, B., Roeder, K. & Wasserman, L. Genomic control, a new approach to genetic-based association studies. *Theor. Popul. Biol.* **60**, 155–166 (2001).
61. de Bakker, P.I. *et al.* Practical aspects of imputation-driven meta-analysis of genome-wide association studies. *Hum. Mol. Genet.* **17**, R122–R128 (2008).
62. Pe'er, I., Yelensky, R., Altshuler, D. & Daly, M.J. Estimation of the multiple testing burden for genomewide association studies of nearly all common variants. *Genet. Epidemiol.* **32**, 381–385 (2008).
63. Johnson, A.D. *et al.* SNAP: a web-based tool for identification and annotation of proxy SNPs using HapMap. *Bioinformatics* **24**, 2938–2939 (2008).
64. Sreejit, P., Kumar, S. & Verma, R.S. An improved protocol for primary culture of cardiomyocyte from neonatal mice. *In Vitro Cell. Dev. Biol. Anim.* **44**, 45–50 (2008).
65. Livak, K.J. & Schmittgen, T.D. Analysis of relative gene expression data using real-time quantitative PCR and the 2(-Delta Delta C(T)) method. *Methods* **25**, 402–408 (2001).
66. Lee, P. *et al.* Conditional lineage ablation to model human diseases. *Proc. Natl. Acad. Sci. USA* **95**, 11371–11376 (1998).